Embryonic development and perinatal skeleton in a limbless, viviparous lizard, *Anguis fragilis* (Squamata: Anguimorpha)

Tomasz Skawiński [Corresp., 1] , **Grzegorz Skórzewski** [2] , **Bartosz Borczyk** [1]

[1] Department of Evolutionary Biology and Conservation of Vertebrates, University of Wroclaw, Wrocław, Poland

[2] Museum of Natural History, University of Wroclaw, Wrocław, Poland

Corresponding Author: Tomasz Skawiński
Email address: tomasz.skawinski@uwr.edu.pl

Despite the long history of embryological studies of squamates, many groups of this huge clade have received only limited attention. One of such understudied groups is anguimorphs, a clade comprising morphologically and ecologically very diverse lizards. We describe several stages of embryonic development of *Anguis fragilis*, a limbless, viviparous anguimorph. Interestingly, in several clutches we observe high morphological variation in characters traditionally important in classifying embryos into developmental stages. The causes of this variation remain unknown but environmental factors do not seem to be very important. Additionally, we describe the state of ossification in several perinatal specimens of *A. fragilis*. The cranial skeleton is relatively poorly ossified around the time of birth, with all of the bones constituting the braincase unfused. On the other hand, the vertebral column is well ossified, with the neurocentral sutures closed and the neural arches fused in all postatlantal vertebrae. Such an advanced state of ossification may be related to the greater importance of the vertebral column in locomotion in limbless species than in ones with fully-developed limbs. Numerous factors seem to affect the state of ossification at the time of hatching or birth in squamates, including phylogenetic position, mode of reproduction and, potentially, limblessness. However, data from a greater number of species are needed to reach firmer conclusions about the relative importance of these variables in certain clades.

1 **Embryonic development and perinatal skeleton in a limbless,**
2 **viviparous lizard, *Anguis fragilis* (Squamata: Anguimorpha)**

3 Tomasz Skawiński[1], Grzegorz Skórzewski[2], Bartosz Borczyk[1]

4 [1] Department of Evolutionary Biology and Conservation of Vertebrates, Faculty of Biological Sciences,
5 University of Wroclaw, Wrocław, Poland

6 [2] Museum of Natural History, Faculty of Biological Sciences, University of Wroclaw, Wrocław, Poland

8 Corresponding Author:

9 Tomasz Skawiński[1]

10 Sienkiewicza 21, Wrocław, 50-335 Wrocław, Poland

11 Email address: tomasz.skawinski@uwr.edu.pl

12   **Abstract**
13   Despite the long history of embryological studies of squamates, many groups of this huge clade
14   have received only limited attention. One of such understudied groups is anguimorphs, a clade
15   comprising morphologically and ecologically very diverse lizards. We describe several stages of
16   embryonic development of *Anguis fragilis*, a limbless, viviparous anguimorph. Interestingly, in
17   several clutches we observe high morphological variation in characters traditionally important in
18   classifying embryos into developmental stages. The causes of this variation remain unknown but
19   environmental factors do not seem to be very important. Additionally, we describe the state of
20   ossification in several perinatal specimens of *A. fragilis*. The cranial skeleton is relatively poorly
21   ossified around the time of birth, with all of the bones constituting the braincase unfused. On the
22   other hand, the vertebral column is well ossified, with the neurocentral sutures closed and the
23   neural arches fused in all postatlantal vertebrae. Such an advanced state of ossification may be
24   related to the greater importance of the vertebral column in locomotion in limbless species than
25   in ones with fully-developed limbs. Numerous factors seem to affect the state of ossification at
26   the time of hatching or birth in squamates, including phylogenetic position, mode of
27   reproduction and, potentially, limblessness. However, data from a greater number of species are
28   needed to reach firmer conclusions about the relative importance of these variables in certain
29   clades.

31   **Introduction**
32   Squamates include over 11,000 living species (Uetz, Freed & Hošek, 2021), which makes them
33   one of the largest clades of extant vertebrates. They live in different environments and show
34   various modifications of their basic body plan, including but not limited to different degrees of
35   limb reduction. The origins of this diversity may be illuminated by studies on embryonic
36   development. The development of squamates has been studied for a long time (e.g., Leydig,
37   1872; de Beer, 1930) and there are numerous publications on the subject. For example,
38   developmental staging tables (some complete, others restricted to certain developmental period
39   or body structure) are available for more than 60 species (see Ollonen et al., 2018). However,
40   some important squamate clades received only a little attention in embryological studies.
41   Anguimorpha, although not particularly species-rich (the group comprises approximately 240
42   currently accepted extant species; Uetz, Freed & Hošek, 2021), are one of the major squamate
43   clades and include morphologically and ecologically very diverse species; limbless burrowers
44   (e.g., *Anniella pulchra*), terrestrial species with fully-developed limbs (some anguids,
45   xenosaurids, helodermas, many species of *Varanus*), and even semiaquatic lizards (some species
46   of *Varanus*, *Shinisaurus crocodilurus* and *Lanthanotus borneensis*) (Pianka & Vitt, 2003).
47   Complete developmental staging tables are available only for three species of monitor lizards
48   (Gregorovicova et al., 2012; Werneburg, Polachowski & Hutchinson, 2015; Andrews et al.,
49   2017) and cranial development of *Elgaria coerulea* (Good, 1995). Such limited data obscure the
50   true variation present within Anguimorpha and hinder large-scale evolutionary analyses of
51   squamate development (e.g., Maisano, 2002; Andrews, Brandley & Greene, 2013; Werneburg &
52   Sánchez-Villagra, 2015; Skawiński & Borczyk, 2017).

53   To fill part of this gap, we studied the development of the slow worm (*Anguis fragilis*), a species
54   of medium-sized, limbless, viviparous anguimorph lizard, widely distributed in Europe (e.g.,

55 Gvoždík et al., 2010, 2013). Even though its early development, from the cleavage to the closure
56 of the amnion, has been thoroughly studied (Nicolas, 1904; Ballowitz, 1905; Meyer, 1910), as
57 well as the genital (Raynaud, 1963) and limb bud development (see review in Raynaud, 1985),
58 only limited attention has been paid to later stages (e.g., Raynaud, 1959). Therefore, many
59 aspects of development in slow worms are still poorly known. Several papers dealt with (or at
60 least commented on) skeletal development but focused only on selected structures or regions
61 such as integument (Maderson, 1965), vertebrae (Winchester & Bellairs, 1977), sacral region
62 (Borkhvardt & Malashichev, 2000) or skull, including the chondrocranium (Leydig, 1872;
63 Zimmermann, 1913; Yaryhin et al., 2021[1]), ethmoidal (Pratt, 1948), orbitotemporal (Bellairs,
64 1949) or frontoparietal (Da Silva et al., 2018) regions. We here supplement these works by
65 providing descriptions of embryo morphology at several stages, as well as perinatal and early
66 postnatal osteology. Information about the neonatal skeleton in squamates are scarce. This is
67 especially true for anguimorphs, for which only data for viviparous anguid *Elgaria coerulea* are
68 available (Maisano, 2001). Its skeleton was poorly ossified and we predict that the degree of
69 skeletal development is similar in perinatal slow worms.

70

71 **Material & Methods**
72 This study is based on five perinatal slow worms and 42 embryos dissected out of 7–9 ethanol-
73 preserved females (the mother is not known in three embryos but they are likely from the same
74 clutch; Table 1, Table S1). These specimens are in collections of the Museum of Natural History
75 (MNHW) or the Department of Evolutionary Biology and Conservation of Vertebrates (IZK),
76 both at the University of Wrocław. The females were identified as *Anguis fragilis* based on
77 morphology (Sos, 2011), and locality when known (all were collected in areas where *A. fragilis*
78 is the only species of *Anguis*; e.g., Jablonski et al., 2017; Table 1). The majority of these females
79 (presumably all) were collected in the field, so the exact age of the embryos can only be
80 approximated based on the date of collection of the mother (Table 1). We assessed the
81 developmental stage of the embryos based on the examination of their morphology under Zeiss
82 Stemi SV 11 stereomicroscope, with particular reference to characters from the Standard Event
83 System (Werneburg, 2009) and those commonly used in developmental tables of squamate
84 embryos. Photographs were taken using Zeiss AxioCam HRc camera mounted on a
85 stereomicroscope. As the embryos are very fragile and many of them were strongly curled, we
86 made all measurements using images. However, because not all developmental stages are
87 represented in our sample, the descriptions below are not equivalent to classical staging tables.
88 For comparison, we used several skeletonised adult and juvenile slow worms (IZK 01004, IZK
89 01005, IZK 01006) and one double-stained adult specimen (MNHW-Reptilia-280).

90 The snout-vent length (SVL) of newly born slow worms varies between 40 and 56 mm (48–49
91 mm on average), based on data from northwestern Spain (Ferreiro & Galán, 2004). Because it
92 was usually unknown whether the specimens in our sample were dissected out of captured
93 females or collected after birth, we refer to them collectively as 'perinatal' (only the largest

---

[1] Based on the geographic origin of their sample (eastern Slovakia), it seems that Yaryhin et al. (2021) studied most probably *Anguis colchica* which used to be regarded as a subspecies of *A. fragilis* but is now considered a distinct, although very closely related, species (e.g., Gvoždík et al., 2010; Speybroeck et al., 2020).

94   specimen, MNHW-Reptilia-0312, with SVL = 55 mm, was collected definitely after birth, and
95   the second-largest specimen, MNHW-Reptilia-0311-1, with SVL = 49 mm, was collected most
96   probably after birth).

97   The perinatal slow worms and a few embryos were double-stained (following the method
98   described by Dingerkus & Uhler, 1977 with slight modifications) to analyse their skeletal
99   development. The specimens were stained with alcian blue for demonstration of cartilage,
100 digested in a sodium borate-pancreatin solution and subsequently stained with alizarin red S to
101 visualise the calcifications. Subsequently, the specimens were transferred through a series of
102 KOH-glycerin solutions and ultimately stored in pure glycerin with the addition of thymol
103 (Dingerkus & Uhler, 1977). In the four smallest perinatal specimens (SVL between 44 and 49
104 mm), which were collected in the 1960s, the alcian blue did not bond to the cartilage, so the
105 descriptions are based entirely on the alizarin-stained calcifications.

106 Complete osteological description of the perinatal skeleton is beyond the scope of the present
107 article (although we acknowledge that such work is desirable in light of recent taxonomic
108 revisions of *Anguis* – Gvoždík et al., 2010, 2013). However, because of the paucity of data on the
109 osteology of slow worms and anguines in general (Rieppel, 1980; Klembara et al., 2017; Villa &
110 Delfino, 2019), we provide a brief description of the "external osteology" of articulated skulls of
111 double-stained specimens. Descriptions of bone morphology are based primarily on the largest
112 and most mature individual (MNHW-Reptilia-0312), while descriptions of ontogenetic changes
113 are based on all double-stained specimens. We put particular emphasis on characters
114 distinguished by Maisano (2001) and known to show interspecific differences in squamates.
115 Identification and nomenclature of bones and other anatomical structures follow the works of
116 Maisano (2001), Evans (2008), Klembara et al. (2017) and Villa & Delfino (2019).

117

Results
Morphology of the embryos
120 **Developmental state 1** (Figure 1A)**.** The posterior neuropore is closed but the anterior one is still
121 open. The somites are impossible to distinguish. The mesencephalon forms a bulge at the back of
122 the head, with its apex located just posterior to the mid-point of the eye. The eye is poorly
123 pigmented. The optic (choroid) fissure is open. The medial nasal processes are separated by a
124 deep midline furrow. The anterior end of the maxillary process lies beneath the anterior part of
125 the eye but does not reach the level of its anterior margin. The tip of the mandibular process lies
126 approximately at the midline of the eye. Only two pharyngeal slits can be distinguished. The
127 cervical flexure is about 90º (Fig. 1A, 2).

128 **Developmental state 2** (Figure 1B)**.** The entire neural tube is closed. The maxillary process
129 fuses with the frontonasal mass which creates an almost continuous upper jaw. The eye is much
130 better pigmented than in the previous stage and the optic fissure can no longer be observed. The
131 tip of the mandibular process reaches the level of the anterior margin of the eye (Fig. 1B).

132 **Developmental states 3-4** (Figure 1C-E)**.** These stages show the greatest variability in
133 morphological traits. Uniformly, all pharyngeal slits are closed and the pupil and eyelid develop.
134 The entire mesencephalic bulge now lies posterior to the eye. The heart is relatively much

135   smaller than in preceding stages but still protrudes from the body cavity. The hemipenes are
136   present (Fig. 3). The variable traits include: disappearance of the cervical flexure, the length of
137   the snout and the length of the mandible. These features can be present in different combinations,
138   for example, the specimen with no cervical flexure may have a mandible significantly shorter
139   than the upper jaw (reaching approximately the anterior margin of the eye) (Figs. 1C, 1D), while
140   others show the cervical flexure, the mandible already reaching the occlusal point with the upper
141   jaw, but the whole snout is very short (Figs. 1C, 1D). For measurements, see Table S1 and Fig.
142   S1. At these stages, no mineralisations in the skeleton could be detected by double-staining (Fig.
143   4).

144   **Developmental state 5** (Figure 1F, 1G)**.** The body is more elongated and the tail is much less
145   curled than in previous stages. In most specimens the snout is as long or slightly longer than the
146   diameter of the eye. The posterior part of the mandible becomes much deeper. The
147   mesencephalon becomes less prominent but still forms a bulge. In some specimens the external
148   nares become easily observable as depressions (Figs. 1F, 1G).

149   **Developmental state 6** (Figure 1H)**.** The lower eyelid reaches the ventral margin of the pupil.
150   The mesencephalon flattens and no longer takes on a bulge-like form. The head is strongly
151   domed in lateral view. The pineal eye develops on the top of the head, approximately at the level
152   of the posterior margin of the eye. Incipient scales develop on the trunk and venter (Fig. 1H). In
153   the skull, several endochondral bones are ossifying: the exoccipital, basioccipital, basisphenoid,
154   quadrate, epipterygoid and articular. With the exception of the exoccipital and basioccipital they
155   only faintly stain with alizarin. Dermal bones tend to be better ossified. The pterygoid, parietal,
156   frontal, prefrontal, squamosal, maxilla, dentary, angular and supraangular are ossified. The
157   parietals are unfused; only their lateral margins are ossified. The maxilla is present only as a
158   small and faint calcification (Fig. 5). In the vertebral column, the neural arches and vertebral
159   centra are present in the cervical and most of the thoracic vertebrae. The more posteriorly located
160   vertebrae are more poorly ossified or absent (Fig. 6).

161   **Developmental state 7** (Figure 1I)**.** In lateral view, the head is much flatter than in the previous
162   stage. The lower eyelid partially covers the ventral part of the pupil. Throat scales develop, while
163   the neck and anterior trunk scales become convex (Fig. 1I).

164   **Developmental state 8** (Figure 1J)**.** Perinatal slow worms look almost exactly like adult
165   individuals (Fig. 1J). Main differences concern colouration. Ontogenetic colour changes were
166   described elsewhere (e.g., Juszczyk, 1974).

167

168   ***Perinatal osteology***
169   *Skull*. The ossification of the skull roof is closer to the "less ossified" extreme described by
170   Maisano (2001). The nasal is a paired bone, with an approximately quadrangular shape. Its
171   anterior end is slightly wider mediolaterally than the posterior one. The nasals contact each other
172   medially only in their posterior parts; anteriorly, they are separated by the nasal process of the
173   premaxilla. The nasal contacts the maxilla and prefrontal laterally and the frontal posteriorly
174   (Figs. 7, 8). The frontal is a paired bone forming a large part of the skull roof. It also creates the
175   dorsal part of the orbit. The frontal is greatly expanded posteriorly, where it meets the parietal.

176   Apart from that, the lateral margins of the bone are approximately straight, there is only a slight
177   narrowing just anterior to the posterior expansion. The frontals are unfused in all studied
178   specimens (Fig. 9) except the largest, in which they began to fuse anteriorly (Fig. 7). In the
179   smallest specimens, the parietal is ossified in its posterior and lateral parts, with the parietal
180   fontanelle being approximately triangular (Fig. 9A). Ossification proceeds also from
181   anterolateral parts towards the midline, along the posterior border of the frontals (Fig. 9B).
182   Additional ossification centres are present around the parietal foramen, from which the
183   ossification spreads anteriorly and posteriorly, so that only parts of the parietal that are located
184   laterally and latero-posteriorly to the parietal foramen remain unossified (Fig. 9C). In the largest
185   specimen, the ossification of the parietal is almost complete, with only a small opening posterior
186   to the parietal foramen still unossified (Fig. 7). The postparietal processes are well-developed
187   and slightly curved ventrally (Fig. 8). The posterior margin is "indented" to form a parietal fossa
188   which contacts the cartilaginous ascending process of the supraoccipital (Fig. 7).

189   The premaxilla creates the most anterior point of the skull. It presents an alveolar plate, which
190   bears teeth, and an ascending nasal process. In the slow worm, the nasal process slightly narrows
191   dorsal to the alveolar plate, then expands laterally, so that its widest point is just below the nasals
192   in anterior view, and then tapers to a point. The nasal process separates the anterior parts of the
193   nasals (Fig. 7). The maxilla creates most of the lateral part of the snout. It is composed of an
194   anterior, posterior and facial processes. The anterior process creates part of the ventral and
195   posteroventral border of the external naris, while the steep and tall facial process forms its
196   posterior border. Dorsally, the facial process contacts the nasal and prefrontal. Posteriorly, it
197   meets the palpebral and lacrimal. The long and low posterior process contacts the lacrimal
198   dorsally and the jugal posterodorsally, and continues below the orbit (Fig. 8).

199   The prefrontal is composed of the main body and a long and narrow orbital process that extends
200   approximately to the narrowest point of the frontal. The prefrontal contacts the maxilla anteriorly
201   and the nasal anteromedially, and separates the palpebral from the frontal (Fig. 7). In the smallest
202   studied perinates, there is a more-or-less elipsoidal foramen between the posterior margin of the
203   facial process of the maxilla and the anterior margin of the prefrontal (Fig. 10). The palpebral is
204   a relatively large bone, with the shape approximating a right triangle in dorsolateral view. It
205   contacts the jugal and lacrimal ventrally, the maxilla anteriorly and the postfrontal dorsally (Figs.
206   7, 8). The jugal is a triradiate bone forming most of the ventral and posterior parts of the orbit. It
207   meets the maxilla and lacrimal anteriorly, and the postfrontal and postorbital posterodorsally.
208   The quadratojugal process is present but small (Fig. 8). It is absent in smaller specimens, with
209   SVL between 44 and 46 mm, so it most probably develops postnatally (Fig. 10). The lacrimal
210   creates most of the anterior margin of the orbit. It contacts the maxilla anteriorly and ventrally,
211   jugal posteroventrally and palpebral dorsally. In lateral view, it appears to be separated from the
212   prefrontal by the maxilla-palpebral contact (Fig. 8). The postfrontal is a triradiate bone forming
213   the posterodorsal part of the orbit. The dorsal process is relatively long and slender, contacting
214   the parietal and frontal. The ventral process is shorter and more robust; ventrally, it meets the
215   jugal and excludes the postorbital from the orbit. The posterior process is deeply bifurcated,
216   extending along the parietal and postorbital (Fig. 7). The postorbital is a simply-shaped bone,
217   extending from the jugal and postfrontal anteriorly to the supratemporal posteriorly. Together

218 with the parietal, postfrontal and supratemporal, it creates a small supratemporal fenestra (Fig.
219 7).

220 The squamosal is of the typical "hockey-stick" shape but the posterior, ventrally curved part is
221 not strongly expanded. The squamosal runs laterally to the postorbital; it also meets the
222 supratemporal posteriorly (Figs. 7, 8). The supratemporal is a splint of bone wedged between the
223 postparietal process of the parietal and the squamosal. Like in the latter bone, its posterior part is
224 curved ventrally (Fig. 8).

225 The quadrate lies lateral to the braincase and together with the articular participates in forming
226 the mandibular joint. The tympanic crest, which extends from the anterodorsal part of the bone to
227 the mandibular condyle, is almost straight. The cephalic condyle is located at the posterodorsal
228 end and almost contacts the squamosal and supratemporal. Dorsally (cephalic condyle) and
229 ventrally (mandibular condyle), the quadrate is still covered by cartilaginous caps (Fig. 8). The
230 epipterygoid is a thin bony rod supported by the pterygoid ventrally and meeting the prootic
231 posterodorsally. In the largest examined specimen, the dorsal end still bears a small cartilaginous
232 cap (Fig. 8).

233 In the palate, the pterygoids are widely separated medially and there is no sign of palatal teeth
234 observed. The pterygoid is an approximately y-shaped bone. The posterior process contacts the
235 quadrate laterally. Medially, the main body contacts the basipterygoid process of the
236 parasphenoid. The anterolateral process of the pterygoid meets the ectopterygoid and the long
237 anterior process contacts the palatine with an almost straight suture (Fig. 11). The palatines are
238 widely separated posteriorly, while the space between them is much smaller anteriorly, where
239 they contact the vomers (Fig. 11). The vomers contact each other at the midline (Fig. 11).

240 In the braincase, only the fusion of the exoccipitals and opisthotics into the otooccipitals takes
241 place prenatally. Other bones remain unfused after birth. Even in the second-largest specimen
242 (MNHW-Reptilia-0311-1, SVL = 49 mm), there are still wide spaces between most of the bones
243 constituting the braincase (Fig. 12). The basicranial fenestra between the basisphenoid and
244 basioccipital persists in the largest neonate examined (Fig. 13). The basioccipital forms the main
245 part of the base of the braincase. In the second-largest specimen, it is approximately U-shaped in
246 ventral view (Fig. 12). Its anterior margin is strongly concave so that the basicranial fenestra is
247 large. Laterally, there is a shallow notch approximately in the mid-length of the bone (Fig. 12).
248 The sphenoid is a composite bone composed of the endochondral basisphenoid and dermal
249 parasphenoid. Both these components are already ossified at the time of birth. The basipterygoid
250 processes have slightly expanded ends which contact the pterygoids in the largest specimen (Fig.
251 13). These two elements are more widely separated in the second-largest slow worm (Fig. 12).
252 The posterior margin of the basisphenoid is not straight in ventral view but bears two shallow
253 notches, near the left and right margins (Fig. 12). The supraoccipital creates the posterodorsal
254 part of the braincase. Laterally, it contacts the postparietal processes of the parietal (more
255 dorsally) and the prootics (more ventrally). Posterolaterally it also contacts the otooccipitals. The
256 anterior margin of the bone is strongly concave in dorsal view, with anterior tips projecting
257 anteriorly. At the midline, there is a cartilaginous ascending process which extends to the parietal
258 fossa. There are two shallow notches in the posterior margin of the bone, near the dorsolateral
259 borders of the foramen magnum, close to the most median contact with the otooccipitals (Fig. 7).

260   The prootic constitutes the lateral part of the braincase. It contacts the parietal dorsally, the
261   supraoccipital posteromedially, the otooccipital posteriorly and the sphenoid ventrally. It has a
262   relatively large, slightly downturned alar process that meets the dorsal part of the epipterygoid.
263   In the largest studied specimen, it has two small tubercles, both in contact with the epipterygoid;
264   one located near the 'apex' of the process and the second, slightly more posterodorsally (Fig. 8).
265   These tubercles were not observed in smaller specimens. The otooccipital forms the
266   posterolateral part of the braincase, as well as the lateral margin of the foramen magnum. In
267   dorsal view, it contacts the prootic anteriorly and the supraoccipital anteromedially. It extends
268   approximately from the posterior end of the supratemporal laterally to the notch in the
269   supraoccipital medially (Fig. 7).

270   The mandible halves are not fused in all studied specimens and Meckel's cartilage persists even
271   in the largest specimen, in which it extends posteriorly almost to the level of the articular surface
272   for the quadrate. Anteriorly, Meckel's cartilages are not fused (Fig. 13). The coronoid is not
273   firmly fused to other mandibular bones (Fig. 8) but otherwise, the morphology of the remaining
274   bones (dentary, angular, surangular, articular) is very similar to the adult form. The articular
275   surface for the quadrate, as well as the posterior end of the retroarticular process, are still capped
276   by cartilage (Fig. 8).

277   Calcified endolymph in dorsal lymphatic sacs within the cranium occurs in only one specimen
278   (Fig. 9B). The scleral ossicles were ossified in all studied specimens (Figs. 8, 10). The
279   ossification of the first ceratobranchial was also completed prenatally. In the largest specimen,
280   the basihyal and hypohyals are calcified (Fig. 13). No calcifications in the trachea or larynx were
281   observed.

282   *Vertebral column*. The ossification of the vertebral column is relatively advanced near the time
283   of birth. Both neural arches are already fused in postatlantal vertebrae of the smallest studied
284   slow worms (MNHW-Reptilia-0310-4 and 0310-5, both with SVL = 44 mm). Similarly, the
285   neurocentral sutures of all vertebrae except the atlas are closed. In the atlas, both neural arches
286   and the centrum remain separate in all studied specimens (Figs. 7, 9). Low neural spines are
287   present even in the smallest specimens and their ossification is almost complete in the largest
288   one, with only the tips still being cartilaginous (Fig. 14). The sacral ribs do not contact one
289   another in any of the studied slow worms.

290   *Limb girdles*. In the pectoral girdle, only the coracoid is ossified in all but the largest studied
291   specimen. It is a small bone with expanded dorsal and especially ventral ends (Fig. 10). In the
292   largest specimen, the expansions further increase. Additionally, a small scapula ossifies dorsal to
293   the coracoid. There is no sign of fusion between these two bones (Fig. 14). In the pelvic girdle of
294   all perinatal specimens, all three pelvic bones could be distinguished which indicates that even
295   the very small pubis and ischium ossify prenatally. The pubis is represented by an anteriorly
296   projecting pubic process, with its anterior end capped by cartilage (although the cartilage was
297   stained only in the largest specimen), and the ischium is present as a posteriorly projecting
298   ischiac process (Fig. 15A, 15B). However, even in the second largest lizard, these two processes
299   are still very small (Fig. 15A).

300

Discussion

301 It is difficult to directly compare the development of *Anguis fragilis* to other anguimorphs
302 because several stages are missing in the sequence of the former species. Although the available
303 data (Gregorovicova et al., 2012; Werneburg, Polachowski & Hutchinson, 2015; Andrews et al.,
304 2017) suggest that the developmental sequences are similar, one of the apparent differences is
305 the timing of appearance of the external nares. In *Varanus indicus* (Gregorovicova et al., 2012)
306 and especially in *V. panoptes* (Werneburg, Polachowski & Hutchinson, 2015), they could be
307 observed at relatively much earlier stages than in *A. fragilis*. The nasal region of the
308 chondrocranium shows a paedomorphic state in *Anguis* (Yaryhin et al., 2021) but it is unclear
309 whether these two features could be linked. Almost certainly it is an artefact of preservation,
310 because the external nares in squamates generally, develop at earlier stages than was observed in
311 our sample of *A. fragilis* (e.g., Kaczmarek, Metscher & Rupik, 2021). In addition, newly-formed
312 external nares are filled by a nasal plug (e.g., Kaczmarek, Metscher & Rupik, 2021) which
313 further hinders their identification.

315 Interestingly, in a few clutches, we observed high variation in characters considered important in
316 developmental tables, such as the disappearance of cervical flexure or mandible length.
317 Therefore, some embryos dissected from a female would be classified in a different stage from
318 some of their siblings (for example, lizards shown in Figure 1C and 1D were dissected from the
319 same female). A similar situation was described in a typhlopid snake *Amerotyphlops*
320 *brongersmianus* (Sandoval, Ruiz García & Álvarez, 2020). In that case, the authors suggest that
321 this variation may result from asynchronous development during the early phase of embryonic
322 development when the effect of external (environmental) factors is the greatest (Sandoval et al.,
323 2020). Indeed, some characters occurring in the early developmental phase were shown to be
324 quite variable in the iguanian *Uta stansburiana* (Andrews & Greene, 2011). Many factors
325 affecting embryonic development have been identified in lizards. Light can significantly
326 accelerate embryonic development (Zhang et al., 2016). However, in viviparous species such as
327 *A. fragilis* the embryos develop within the body cavity of the female. This also would not explain
328 the variation within a single clutch. Temperature is another factor because higher temperatures
329 usually accelerate development (Noble, Stenhouse & Schwanz, 2018). The temperature within
330 the animal body is not identical in different parts (e.g., Schmidt-Nielsen, 1997), so it seems
331 possible that embryos developing closest to heat-producing organs such as heart or stomach
332 would be in a slightly more advanced stage of development when compared to embryos
333 developing in slightly cooler places. Unfortunately, information about the topographic position
334 of given embryos within the female body is not always available. Also, in most of the clutches,
335 the morphological differences between embryos are minimal. Thus, the effect of temperature on
336 this variation, if any, seems to be very limited. Embryonic development may also be affected by
337 the availability of oxygen in the oviducts, which is smaller in larger clutches (Foucart, Heulin &
338 Lourdais, 2017), but our data are too limited to tell whether this may be the case in *A. fragilis*.
339 Importantly, we observed the variation in later stages than was reported in *Am. brongersmianus*
340 (Sandoval, Ruiz García & Álvarez, 2020), when the effect of the environment is presumed to be
341 smaller. Therefore, it cannot be excluded that some intrinsic, genetic factors could play a role.
342 One of the potential explanations is multiple paternity which affects the time of fertilisation and,
343 therefore, the age of the embryos. Such small differences in age could be reflected in the
344 morphology of the embryos. Although multiple paternity has not yet been reported for *A.*

345 *fragilis*, this phenomenon is known to occur widely in reptiles (Uller & Olsson, 2008).
346 Additionally, multiple paternity is usually present only in a fraction of the clutches in a given
347 population or species (Uller & Olsson, 2008). This would be consistent with the fact that only
348 some clutches of *A. fragilis* showed such phenotypic variation. We aim to test this hypothesis in
349 a forthcoming contribution.

350 The degree of calcification in the vertebral column in a late embryo (developmental state 6)
351 indicates an anteroposterior order of ossification in the postcranial axial skeleton. This pattern is
352 predominant in squamates (e.g., Hugi et al., 2012; Roscito & Rodrigues, 2012), however, in
353 another anguimorph, *Varanus panoptes*, all vertebrae seem to ossify nearly simultaneously,
354 without a clear gradient (Werneburg, Polachowski & Hutchinson, 2015). The dermatocranium
355 develops earlier than the neurocranium in *A. fragilis*, an almost universal feature in squamates
356 (Evans, 2008). This state 6 embryo seems to be at an earlier developmental stage than the one
357 illustrated by Leydig (1872), as indicated by the lack of the ossified palatine, premaxilla and
358 vomer. Interestingly, we observed only a small and faint ossification in the maxilla (while the
359 other tooth-bearing bone of the upper jaw, the premaxilla, is absent). Thus, the maxilla seems to
360 ossify relatively later in *A. fragilis* than it does in other studied anguimorphs, *Elgaria coerulea*
361 and *V. panoptes* (Good, 1995; Werneburg, Polachowski & Hutchinson, 2015). On the other
362 hand, the ossification of the articular is accelerated in *A. fragilis* in comparison to *E. coerulea*, in
363 which it is the last cranial bone to ossify (Good, 1995).

364 Several aspects of the skeletal anatomy of *A. fragilis* were controversial for many years. For
365 example, the episternum (interclavicle) was described as being variably present in slow worms
366 (Fürbringer, 1870; Krieg, 1919), while Stokely (1947) failed to detect any such ossification. Our
367 observations agree with those of Stokely – in none of the individuals in our sample, either
368 embryonic, perinatal or adult, was this bone present. As Stokely (1947), we also did not observe
369 any sign of the sternum – either cartilaginous or ossified – in *A. fragilis*.

370 The skull of the perinatal slow worms is relatively poorly ossified. None of the braincase bone
371 fusions listed by Maisano (2001) was observed in *A. fragilis*. This is similar to the viviparous
372 gerrhonotine *Elgaria coerulea* which is also characterised by a poorly fused neonatal skull
373 (Maisano, 2001). However, *A. fragilis* shows better ossified parietals because even in the
374 smallest specimens in our sample the parietals were already fused posteriorly and some parts of
375 the parietal table were ossified as well, in contrast to *E. coerulea* in which only lateral margins
376 were ossified (Maisano, 2001). The pattern of parietal ossification also seems to be different
377 between these two species. In *A. fragilis* the centrally-located parts of the bone (laterally and
378 posterolaterally to the parietal foramen) are the last to ossify, while in *E. coerulea* the most
379 anterior part of the bone (which contacts the frontals) is the last (Maisano, 2001). Maisano
380 (2001) hypothesised that such poor ossification of the neonatal skeleton in *E. coerulea* may be
381 related to the viviparity of this lizard because viviparous lizards tend to have more poorly
382 ossified skeletons at the time of birth than do oviparous ones. Data from *A. fragilis* are consistent
383 with this pattern. Additionally, a late embryo of an oviparous monitor lizard, *Varanus panoptes*,
384 has a much better-ossified skull than do both *E. coerulea* and *A. fragilis*. In *V. panoptes*, the
385 ossification of the frontals and parietal is almost complete prenatally, while in the braincase, at
386 least the basioccipital and otooccipitals seem to be fused, based on published figures
387 (Werneburg, Polachowski & Hutchinson, 2015). On the other hand, the frontoparietal region of a

388   late embryo of a viviparous diploglossine (or diploglossid) *Celestus costatus* is better ossified
389   than in neonates of *A. fragilis* or *E. coerulea* (Da Silva et al., 2018). However, the latter two
390   species are more closely related to each other than to *C. costatus* (e.g., Wiens & Slingluff, 2001;
391   Conrad et al., 2011), so the effect of phylogeny also cannot be ruled out. Therefore, a link
392   between viviparity and skeletally immature neonates is not unambiguous and still more data are
393   needed. Interestingly, the vertebral column of *A. fragilis* is well-developed in comparison to most
394   other studied squamates (Maisano, 2001). The neurocentral suture of all vertebrae except the
395   atlas is closed, the neural arches are fused and the neural spines are ossified. In an extensive
396   study, all these three characters were present in neonates only in the amphisbaenian *Bipes*
397   *biporus*, which has robust forelimbs but lacks hindlimbs (Maisano, 2001). Obviously, in limbless
398   or almost limbless squamates, the vertebral column is the most important part of the skeletal
399   system that plays a role in locomotion (e.g., Gans, 1962). Because neonates must be able to
400   move immediately after hatching or birth, it seems logical that the vertebral column would be
401   more strongly ossified in limbless taxa than in species with well-developed limbs. This is
402   consistent with the observation that in skinks with reduced limbs the cervical vertebrae ossify
403   earlier (Hugi et al., 2012). However, this conclusion must remain tentative because the number
404   of studied squamate species (especially limbless ones) is still not sufficient (unfortunately,
405   descriptions of the vertebral column in late embryos of two gymnophthalmids with strongly-
406   reduced limbs, *Calyptommatus sinebrachiatus* and *Nothobachia ablephara*, are not explicit
407   enough to enable more detailed comparisons with *A. fragilis*; Roscito & Rodrigues, 2012).
408   Regardless of these problems, it seems that the state of ossification of the neonatal skeleton in
409   squamates is a result of trade-offs between numerous variables such as phylogeny, ovi- or
410   viviparity, and potentially limblessness.

411

Conclusions

412
413   We described several stages of embryonic development in *Anguis fragilis* which represent early,
414   middle and late developmental phases. This represents a starting point for future studies on the
415   development of this species, especially with more densely-sampled late developmental phases.
416   Interestingly, within a few clutches, we observed a high variation in morphological characters
417   which are often considered important in the classification of embryos into stages. The causes of
418   this variation remain unknown but one of the potential explanations may be multiple paternity
419   which affects the time of fertilisation and thus may cause slight morphological differences
420   between individuals from the same clutch.

421   The perinatal cranium is relatively poorly ossified. No fusions in the braincase could be observed
422   even in the largest examined lizard. The frontals are unfused (only in the largest specimen have
423   they started to fuse anteriorly), and the parietal is ossified mostly in lateral and posterior parts.
424   However, the state of ossification seems to be at a more advanced stage than in another
425   viviparous anguid, *Elgaria coerulea*. In contrast to the skull, the vertebral column is well ossified
426   at the time of birth which may be related to the greater importance of the spine in locomotion in
427   limbless species. The state of ossification at the time of hatching or birth in squamates is
428   probably affected by trade-offs between numerous factors, including phylogenetic position,
429   mode of reproduction and, potentially, limblessness. However, studies on a greater number of

430 species are necessary to gain better understanding of the importance of these variables in
431 different clades.

432

433 **Acknowledgements**
434 We are very grateful to Paweł Kaczmarek (University of Silesia in Katowice) for constructive
435 comments on an earlier version of the manuscript and for numerous fruitful discussions about
436 embryology. We thank Beata Rozenblut-Kościsty, Mikołaj Kaźmierczak and Krzysztof Kolenda
437 (University of Wrocław) for help with taking the photographs. We greatly appreciate numerous
438 constructive comments made by Jessica Maisano and Oleksandr Yaryhin which improved the
439 quality of the article. We thank John R. Hutchinson for handling the review process.

440

441 **References**
442 Andrews RM, Brandley MC, Greene VW. 2013. Developmental sequences of squamate reptiles
443 are taxon specific. *Evolution & Development* 15:326–343 DOI: 10.1111/ede.12042.

444 Andrews RM, Greene VW. 2011. Character variation in embryonic development of the lizard
445 *Uta stansburiana*. *Journal of Herpetology* 45:451–454 DOI: 10.1670/10-312.1.

446 Andrews RM, Pezaro N, Doody JS, Guarino F, Green B. 2017. Oviposition to hatching:
447 development of *Varanus rosenbergi*. *Journal of Herpetology* 51:396–401 DOI: 10.1670/16-124.

448 Ballowitz E. 1905. Die Gastrulation bei der Blindschleiche (*Anguis fragilis* L.). *Zeitschrift für*
449 *wissenschaftliche Zoologie* 83:707–732.

450 Bellairs Ad'A. 1949. The anterior brain-case and interorbital septum in Sauropsida, with a
451 consideration on the origin of snakes. *Journal of the Linnean Society of London, Zoology*
452 41:482–512 DOI: 10.1111/j.1096-3642.1940.tb02418.x.

453 Borkhvardt VG, Malashichev YB. 2000. Correlative changes during early morphogenesis of the
454 sacroiliac complex in squamate reptiles. *Annals of Anatomy* 182:439–444 DOI: 10.1016/S0940-
455 9602(00)80050-3.

456 Conrad JL, Ast JC, Montanari S, Norell MA. 2011. A combined evidence phylogenetic analysis
457 of Anguimorpha (Reptilia: Squamata). *Cladistics* 27:230–277 DOI: 10.1111/j.1096-
458 0031.2010.00330.x.

459 Da Silva F, Fabre A-C, Savriama Y, Ollonen J, Mahlow K, Herrel A, Müller J, Di-Poï N. 2018.
460 The ecological origins of snakes as revealed by skull evolution. *Nature Communications* 9:376
461 DOI: 10.1038/s41467-017-02788-3.

462 de Beer GR. 1930. The early development of the chondrocranium of the lizard. *Quarterly*
463 *Journal of Microscopical Science* s2-73:707–739.

464 Dingerkus G, Uhler LD. 1977. Enzyme clearing of Alcian blue stained whole small vertebrates
465 for demonstration of cartilage. *Stain Technology* 52:229–232 DOI:
466 10.3109/10520297709116780.

467 Evans SE. 2008. The skull of lizards and tuatara. In: Gans C, Gaunt AS, Adler K, eds. *Biology of*
468 *the Reptilia. Volume 20. Morphology H*. Ithaca: Society for the Study of Amphibians and
469 Reptiles, 1–347.

470 Ferreiro R, Galán P. 2004. Reproductive ecology of the slow worm (*Anguis fragilis*) in the
471 northwest Iberian Peninsula. *Animal Biology* 54:353–371 DOI: 10.1163/1570756042729528.

472 Foucart T, Heulin B, Lourdais O. 2017. Clutch size influences embryonic stages at oviposition in
473 a lizard with prolonged egg retention. *Amphibia-Reptilia* 38:557–561 DOI: 10.1163/15685381-
474 00003128.

475 Fürbringer M. 1870. *Die Knochen und Muskeln der Extremitäten bei den schlangenähnlichen*
476 *Sauriern: vergleichend-anatomische Abhandlung*. Leipzig: Verlag von Wilhelm Engelmann
477 DOI: 10.11588/diglit.3471.

478 Gans C. 1962. Terrestrial locomotion without limbs. *American Zoologist* 2:167–182.

479 Good DA. 1995. Cranial ossification in the northern alligator lizard, *Elgaria coerulea*
480 (Squamata, Anguidae). *Amphibia-Reptilia* 16:157–166 DOI: 10.1163/156853895X00334.

481 Gregorovicova M, Zahradnicek O, Tucker AS, Velensky P, Horacek I. 2012. Embryonic
482 development of the monitor lizard, *Varanus indicus*. *Amphibia-Reptilia* 33:451–468 DOI:
483 10.1163/15685381-00002849.

484 Gvoždík V, Benkovský N, Crottini A, Bellati A, Moravec J, Romano A, Sacchi R, Jandzik D.
485 2013. An ancient lineage of slow worms, genus *Anguis* (Squamata: Anguidae), survived in the
486 Italian Peninsula. *Molecular Phylogenetics and Evolution* 69:1077–1092 DOI:
487 10.1016/j.ympev.2013.05.004.

488 Gvoždík V, Jandzik D, Lymberakis P, Jablonski D, Moravec J. 2010. Slow worm, *Anguis*
489 *fragilis* (Reptilia: Anguidae) as a species complex: genetic structure reveals deep divergences.
490 *Molecular Phylogenetics and Evolution* 55:460–472 DOI: 10.1016/j.ympev.2010.01.007.

491 Hugi J, Hutchinson MN, Koyabu D, Sánchez-Villagra MR. 2012. Heterochronic shifts in the
492 ossification sequences of surface- and subsurface-dwelling skinks are correlated with the degree
493 of limb reduction. *Zoology* 115:188–198 DOI: 10.1016/j.zool.2011.10.003.

494 Jablonski D, Najbar B, Grochowalska R, Gvoždík V, Strzała T. 2017. Phylogeography and
495 postglacial colonization of Central Europe by *Anguis fragilis* and *Anguis colchica*. *Amphibia-*
496 *Reptilia* 38:562–569 DOI: 10.1163/15685381-00003133.

497 Juszczyk W. 1974. *Płazy i gady krajowe*. Warszawa: PWN.

498 Kaczmarek P, Metscher B, Rupik W. 2021. Embryology of the naso-palatal complex in Gekkota
499 based on detailed 3D analysis in *Lepidodactylus lugubris* and *Eublepharis macularius*. *Journal*
500 *of Anatomy* 238:249–287 DOI: 10.1111/joa.13312.

501 Klembara J, Dobiašová K, Hain M, Yaryhin O. 2017. Skull anatomy and ontogeny of legless
502 lizard *Pseudopus apodus* (Pallas, 1775): heterochronic influences on form. *Anatomical Record*
503 300:460–502 DOI: 10.1002/ar.23532.

504   Krieg H. 1919. Beiträge zur Rudimentierungsfrage nach Beobachtungen an *Anguis fragilis*,
505   *Chalcides tridactylus* und *Lacerta serpa*. *Archiv für Entwicklungsmechanik der Organismen*
506   45:571–601 DOI: 10.1007/BF02554410.

507   Leydig F. 1872. *Die in Deutschland lebenden Arten der Saurier*. Tübingen: Verlag der H.
508   Laupp'schen Buchhandlung.

509   Maderson PFA. 1965. The embryonic development of the squamate integument. *Acta Zoologica*
510   46:275–295 DOI: 10.1111/j.1463-6395.1965.tb00735.x.

511   Maisano JA. 2001. A survey of state of ossification in neonatal squamates. *Herpetological*
512   *Monographs* 15:135–157 DOI: 10.2307/1467041.

513   Maisano JA. 2002. The potential utility of postnatal skeletal developmental patterns in squamate
514   phylogenetics. *Zoological Journal of the Linnean Society* 136:277–313 DOI: 10.1046/j.1096-
515   3642.2002.00033.x.

516   Meyer E. 1910. Über die Entwicklung der Blindschleiche (*Anguis fragilis* L.) vom Auftreten des
517   Proamnion bis zum Schlusse der Amnion. *Zeitschrift für wissenschaftliche Zoologie* 94:447–487.

518   Nicolas A. 1904. Recherches sur l'embryologie des reptiles. IV. La segmentation chez l'orvet.
519   *Archives de Biologie* 20:611–658.

520   Noble DWA, Stenhouse V, Schwanz LE. 2018. Developmental temperatures and phenotypic
521   plasticity in reptiles: a systematic review and meta-analysis. *Biological Reviews* 93:72–97 DOI:
522   10.1111/brv.12333.

523   Ollonen J, Da Silva FO, Mahlow K, Di-Poï N. 2018. Skull development, ossification pattern, and
524   adult shape in the emerging lizard model organism *Pogona vitticeps*: a comparative analysis with
525   other squamates. *Frontiers in Physiology* 9:278 DOI: 10.3389/fphys.2018.00278.

526   Pianka ER, Vitt LJ. 2003. *Lizards: windows to the evolution of diversity*. Berkeley: University of
527   California Press.

528   Pratt CWM. 1948. The morphology of the ethmoidal region of *Sphenodon* and lizards. *Journal of*
529   *Zoology* 118:171–201 DOI: 10.1111/j.1096-3642.1948.tb00372.x.

530   Raynaud A. 1959. Développement et croissance des embryons d'Orvet (*Anguis fragilis* L.) dans
531   l'oeuf incubé *in vitro*. *Comptes rendus hebdomadaires des séances de l'Académie des sciences*
532   249:1813–1815.

533   Raynaud A. 1963. Le développement et la différenciation au cours de la vie embryonnaire des
534   ébauches phalliques de l'orvet (*Anguis fragilis* L.). *Comptes rendus hebdomadaires des séances*
535   *de l'Académie des sciences* 257:2721–2724.

536   Raynaud A. 1985. Development of limbs and embryonic limb reduction. In: Gans C, Billet F,
537   eds. *Biology of the Reptilia. Volume 15. Development B*. New York, Chichester, Brisbane,
538   Toronto, Singapore: John Wiley & Sons, 59–148.

539   Rieppel O. 1980. The phylogeny of anguinomorph lizards. *Denkschriften der Schweizerischen*
540   *Naturforschenden Gesellschaft* 94:1–86 DOI: 10.1007/978-3-0348-9372-5.

541 Roscito JG, Rodrigues MT. 2012. Skeletal development in the fossorial gymnophthalmids
542 *Calyptommatus sinebrachiatus* and *Nothobachia ablephara*. *Zoology* 115:289–301 DOI:
543 10.1016/j.zool.2012.02.004.

544 Sandoval MT, Ruiz García JA, Álvarez BB. 2020. Intrauterine and post-ovipositional embryonic
545 development of *Amerotyphlops brongersmianus* (Vanzolini, 1976) (Serpentes: Typhlopidae)
546 from northeastern Argentina. *Journal of Morphology* 281:523–535 DOI:10.1111/jmor.21119.

547 Schmidt-Nielsen K. 1997. *Animal physiology: adaptation and environment*. Cambridge:
548 Cambridge University Press.

549 Skawiński T, Borczyk B. 2017. Evolution of developmental sequences in lepidosaurs. *PeerJ*
550 5:e3262 DOI: 10.7717/peerj.3262.

551 Sos T. 2011. Evaluating the accuracy of morphological traits used in *Anguis* (sub)species
552 differentiation. *Herpetologica Romanica* 4:29–44.

553 Speybroeck J, Beukema W, Dufresnes C, Fritz U, Jablonski D, Lymberakis P, Martínez-Solano
554 I, Razzetti E, Vamberger M, Vences M, Vörös J, Crochet P-A. 2020. Species list of the European
555 herpetofauna – 2020 update by the Taxonomic Committee of the Societas Europaea
556 Herpetologica. *Amphibia-Reptilia* 41:139–189 DOI: 10.1163/15685381-bja10010.

557 Stokely PS. 1947. Limblessness and correlated changes in the girdles of a comparative
558 morphological series of lizards. *The American Midland Naturalist* 38:725–754 DOI:
559 10.2307/2421690.

560 Uetz P, Freed P, Hošek J, eds. 2021. The reptile database. *Available at http://reptile-
561 database.org* (accessed 4 May 2021).

562 Uller T, Olsson M. 2008. Multiple paternity in reptiles: patterns and processes. *Molecular
563 Ecology* 17:2566–2580 DOI: 10.1111/j.1365-294X.2008.03772.x.

564 Villa A, Delfino M. 2019. A comparative atlas of the skull osteology of European lizards
565 (Reptilia: Squamata). *Zoological Journal of the Linnean Society* 187:829–928 DOI:
566 10.1093/zoolinnean/zlz035.

567 Werneburg I. 2009. A standard system to study vertebrate embryos. *PLoS ONE* 4:e5887 DOI:
568 10.1371/journal.pone.0005887.

569 Werneburg I, Polachowski KM, Hutchinson MN. 2015. Bony skull development in the Argus
570 monitor (Squamata, Varanidae, *Varanus panoptes*) with comments on developmental timing and
571 adult anatomy. *Zoology* 118:255–280 DOI: 10.1016/j.zool.2015.02.004.

572 Werneburg I, Sánchez-Villagra MR. 2015. Skeletal heterochrony is associated with the
573 anatomical specializations of snakes among squamate reptiles. *Evolution* 69:254–263 DOI:
574 10.1111/evo.12559.

575 Wiens JJ, Slingluff JL. 2001. How lizards turn into snakes: a phylogenetic analysis of body-form
576 evolution in anguid lizards. *Evolution* 55:2303–2318 DOI: 10.1111/j.0014-3820.2001.tb00744.x.

577   Winchester L, Bellairs Ad'A. 1977. Aspects of vertebral development in lizards and snakes.
578   *Journal of Zoology* 181:495–525 DOI: 10.1111/j.1469-7998.1977.tb03259.x.

579   Yaryhin O, Klembara J, Pichugin Y, Kaucka M, Werneburg I. 2021. Limb reduction in squamate
580   reptiles correlates with the reduction of the chondrocranium: a case study on serpentiform
581   anguids. *Developmental Dynamics* Epub ahead of print 15 February 2021 DOI:
582   10.1002/dvdy.307.

583   Zhang Y, Li S, Ping J, Li S, Zhou H, Sun B, Du W. 2016. The effects of light exposure during
584   incubation on embryonic development and hatchling traits in lizards. *Scientific Reports* 6:38527
585   DOI: 10.1038/srep38527.

586   Zimmermann S. 1913. Das Chondrocranium von *Anguis fragilis*. *Anatomischer Anzeiger*
587   44:594–606.

Figure 1

Embryonic development of *Anguis fragilis*.

Lateral view of *A. fragilis* embryos at various developmental states. (A) State 1. (B) State 2. (C-E) States 3-4. (F-G) State 5. (H) State 6. (I) State 7. (J) State 8 (perinate). Scale bar = 2 mm (A-I) or 5 mm (J).

Figure 2

Morphological details of an *Anguis fragilis* embryo.

Head of the state 1 embryo in right (A) and left (B) lateral views. Scale bar = 1 mm. Abbreviations: anp, anterior neuropore; mdp, mandibular process; mnp, medial nasal process; msc, mesencephalon; mxp, maxillary process; of, optic (choroid) fissure; *, pharyngeal cleft.
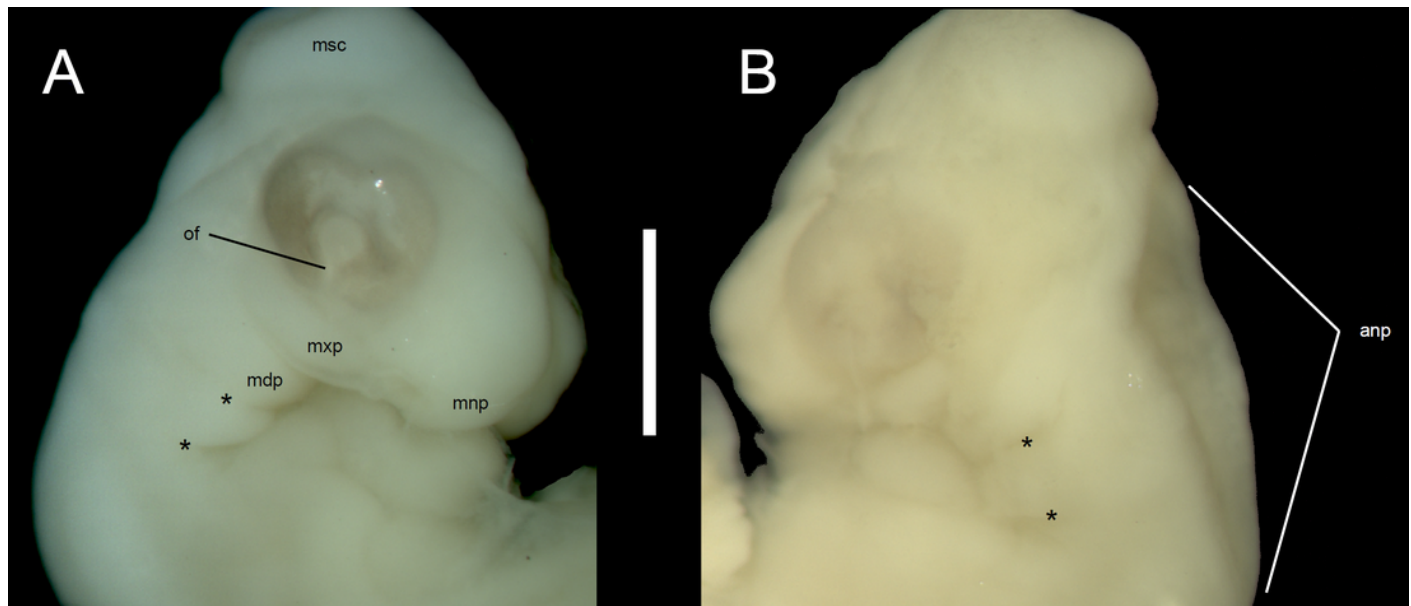
Figure 3

Morphological details of an *Anguis fragilis* embryo.

The snout and incipient hemipenis (hp) of the state 3-4 embryo in lateral view. Scale bar = 1 mm.
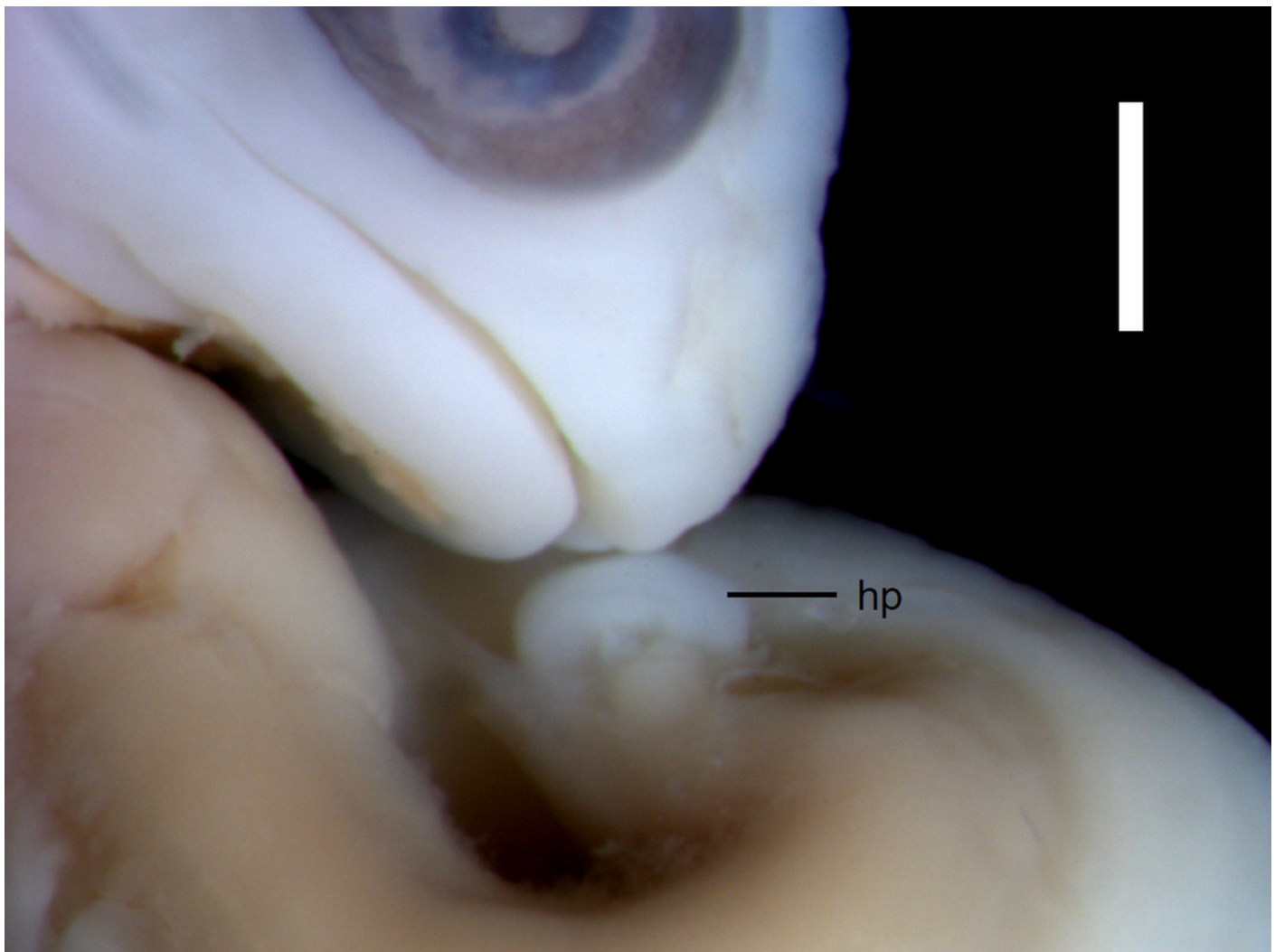
Figure 4

Cartilaginous skeleton of a state 3-4 embryo of *Anguis fragilis*.

Scale bar = 2 mm.

Figure 5

Skull of the double-stained state 6 embryo of *Anguis fragilis*.

(A) Lateral view. (B) Dorsal view. Cartilage is stained bluish while bone is stained red. Scale bar = 2 mm. Abbreviations: art, articular; bo, basioccipital; bs, basisphenoid; d, dentary; eo, exoccipital; ept, epipterygoid; f, frontal; p, parietal; pt, pterygoid; q, quadrate; sq, squamosal. Note that the specimen is not fully articulated.
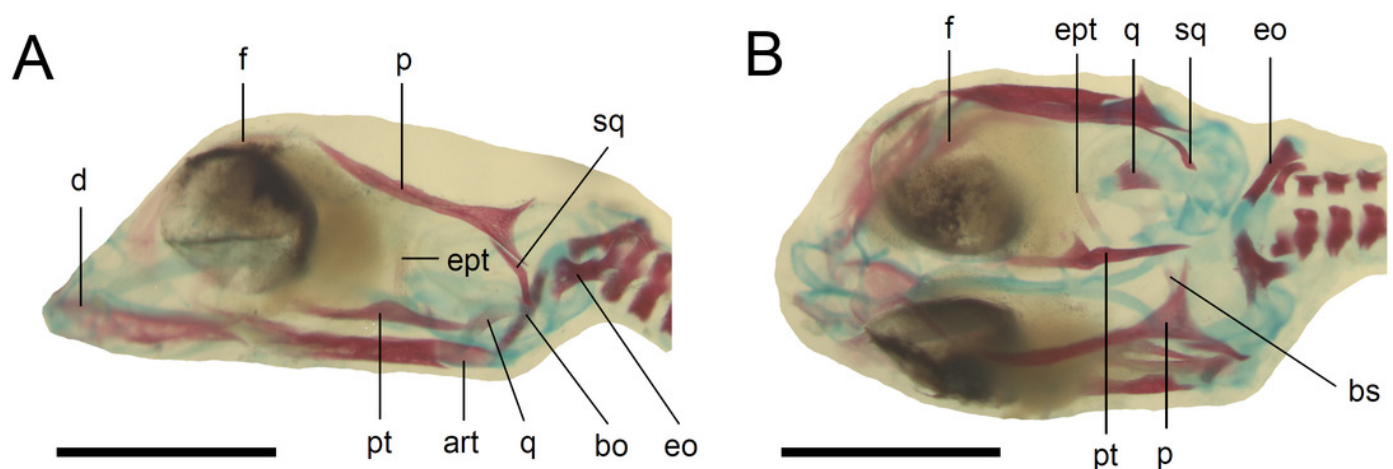
Figure 6

Double-stained state 6 embryo of *Anguis fragilis* in dorsal view.

Cartilage is stained bluish while bone is stained red. Note that the cranium is not fully articulated. Scale bar = 2 mm.

Figure 7

Skull of perinatal *Anguis fragilis* (MNHW-Reptilia-0312) in dorsal view.

Scale bar = 2 mm. Abbreviations: asc, ascending process of the supraoccipital; at, atlas; f, frontal; j, jugal; mx, maxilla; n, nasal; ot, otooccipital; p, parietal; pmx, premaxilla; po, postorbital; pp, postparietal process of the parietal; prf, prefrontal; sco, scleral ossicles; so, supraoccipital; sq, squamosal; st, supratemporal; 1, palpebral; 2, postfrontal.
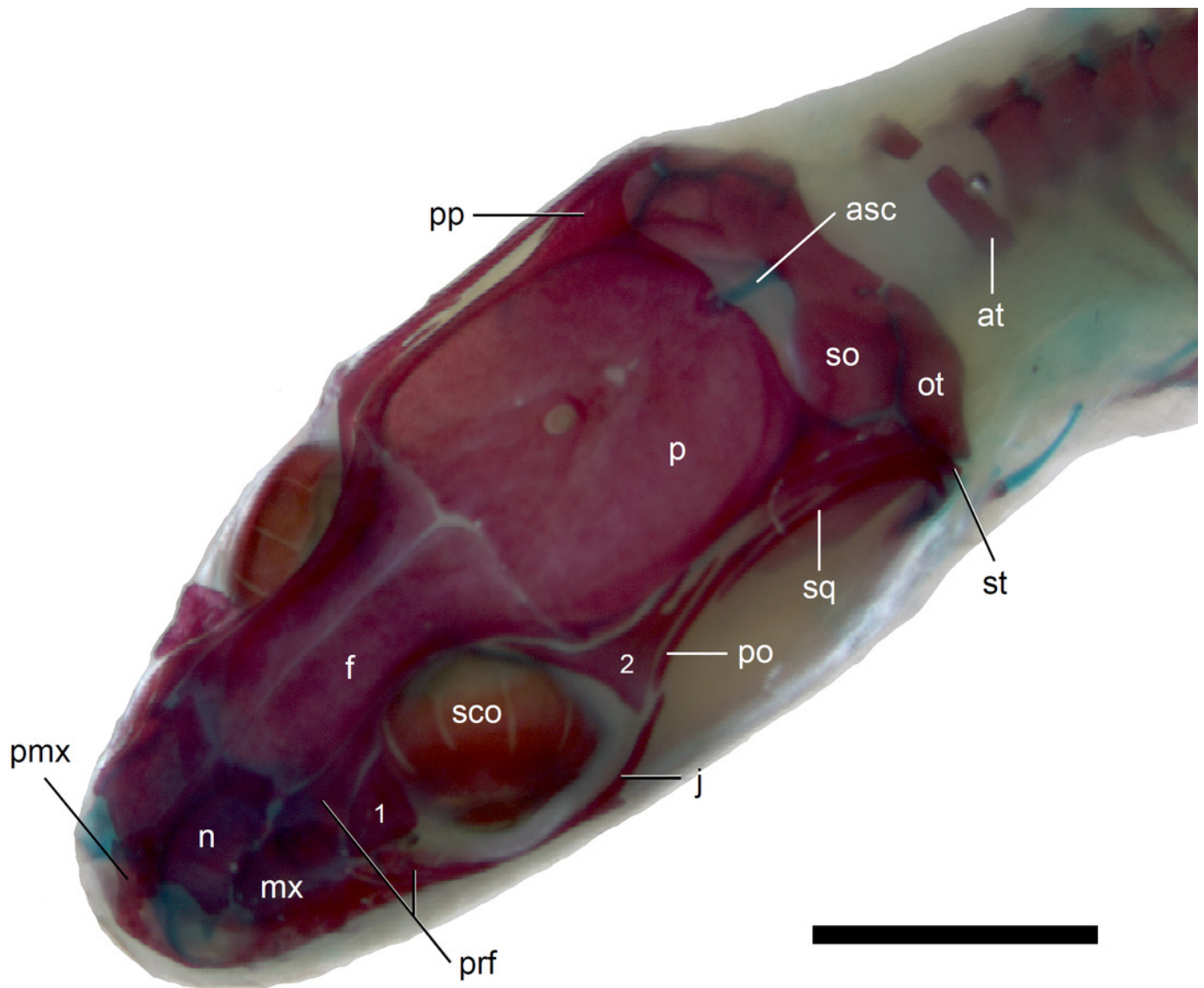
Figure 8

Skull of perinatal *Anguis fragilis* (MNHW-Reptilia-0312) in lateral view.

Scale bar = 2 mm. Abbreviations: asa, articular surface of the articular; ept, epipterygoid; f, frontal; j, jugal; l, lacrimal; mdb, mandible; mx, maxilla; n, nasal; ot, otooccipital; p, parietal; pmx, premaxilla; po, postorbital; prf, prefrontal; pro, prootic; q, quadrate; sco, scleral ossicles; so, supraoccipital; sq, squamosal; 1, palpebral; 2, postfrontal; 3, coronoid.
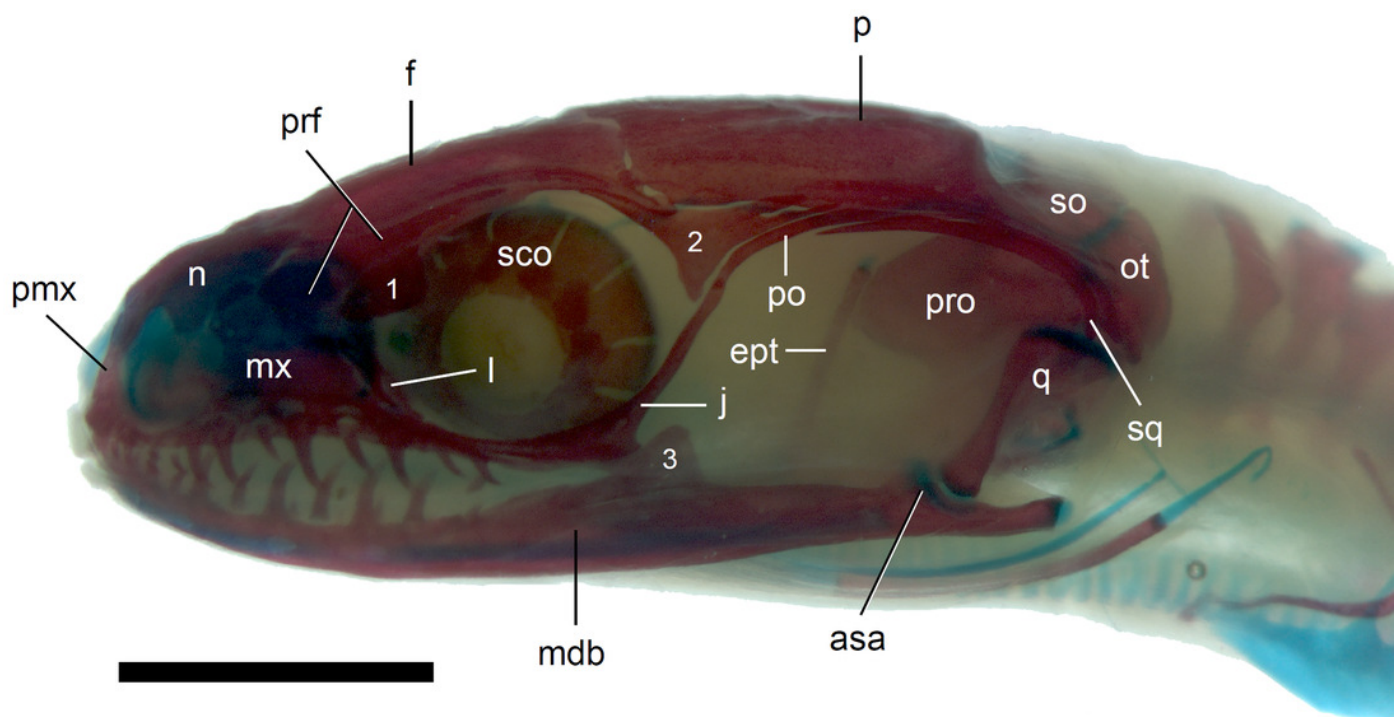
Figure 9

Development of the skull roof in perinatal *Anguis fragilis* in dorsal view.

(A) MNHW-Reptilia-0310-4 (SVL = 44 mm), (B) MNHW-Reptilia-0310-6 (SVL = 46 mm), (C) MNHW-Reptilia-0311-1 (SVL = 49 mm). Scale bar = 2 mm. Abbreviations: ce, calcified endolymph; f, frontal; n, nasal; p, parietal, prf, prefrontal.
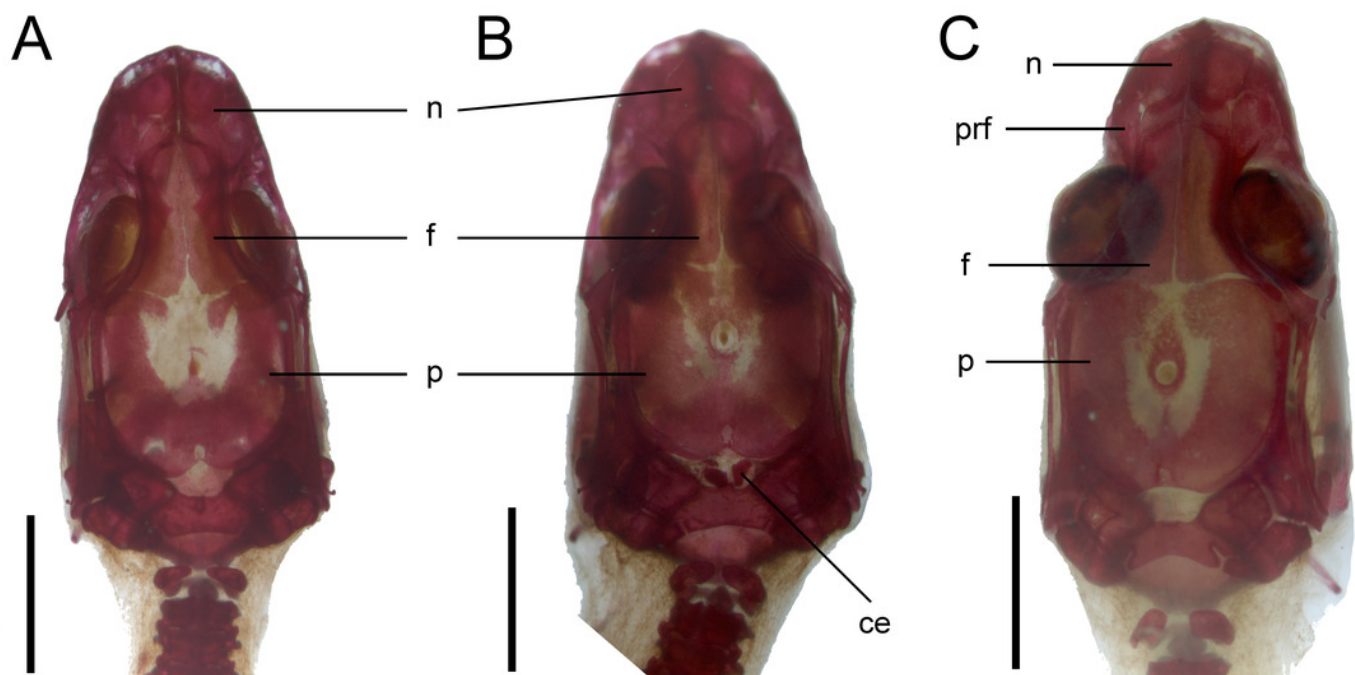
Figure 10

Skull of perinatal *Anguis fragilis* (MNHW-Reptilia-0310-4) in lateral view.

Scale bar = 2 mm. Abbreviations: cb, first ceratobranchial; cl, clavicle; co, coracoid; j, jugal; mx, maxilla; prf, prefrontal; pro, prootic.
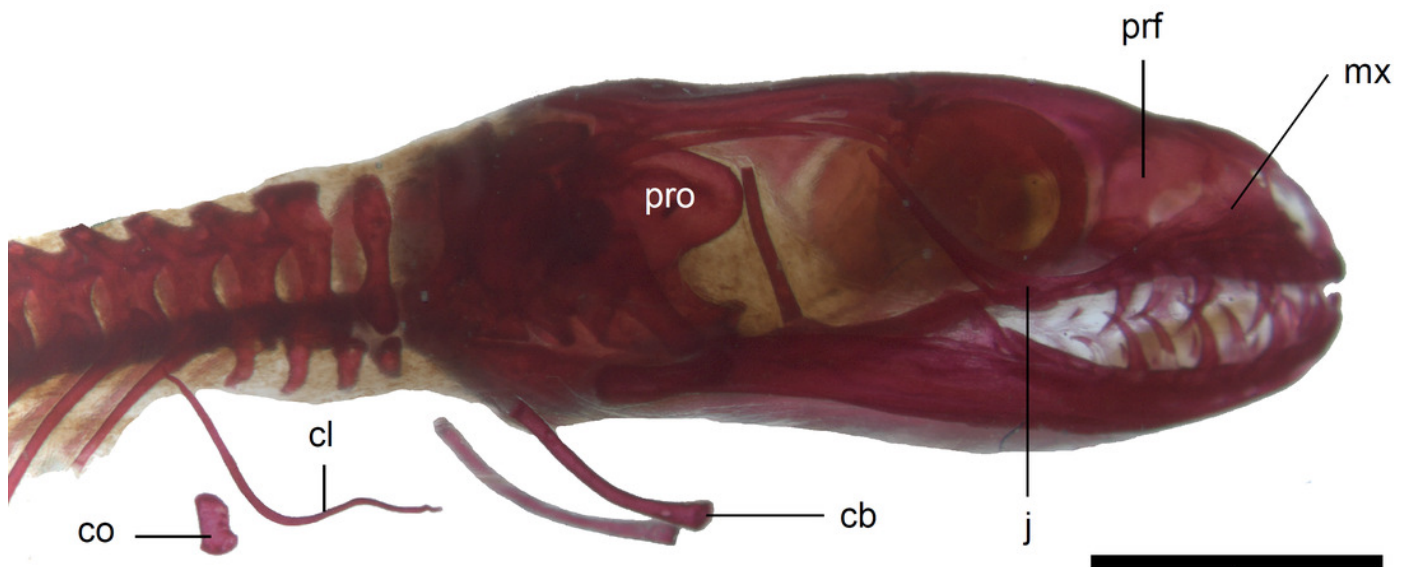
Figure 11

Skull of perinatal *Anguis fragilis* (MNHW-Reptilia-0310-4) in ventral view.

Scale bar = 2 mm. Abbreviations: bo, basioccipital; bs, basisphenoid; ot, otooccipital; pa, palatine; pro, prootic; ps, parasphenoid; pt, pterygoid; v, vomer.
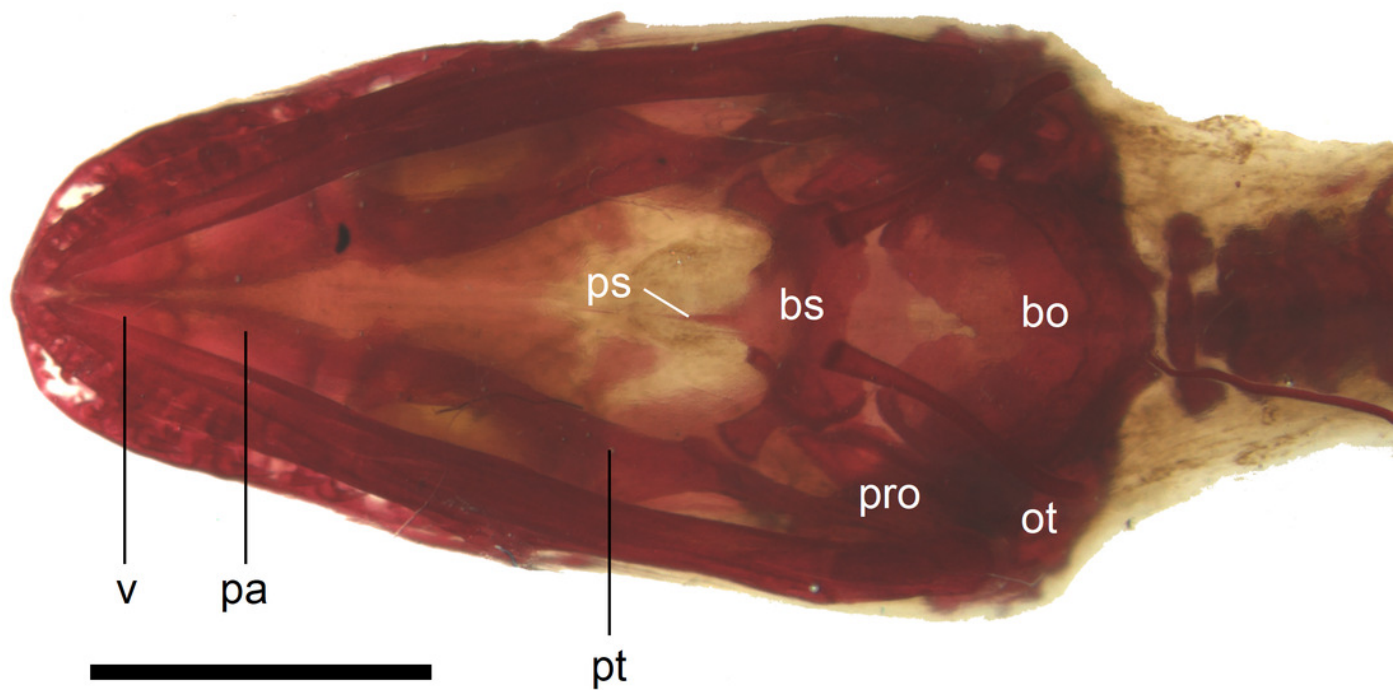
Figure 12

Braincase of perinatal *Anguis fragilis* (MNHW-Reptilia-0311-1) in ventral view.

Scale bar = 1 mm. Abbreviations: bo, basioccipital; bs, basisphenoid; cb, first ceratobranchial; mdb, mandible; pro, prootic; ps, parasphenoid; pt, pterygoid.
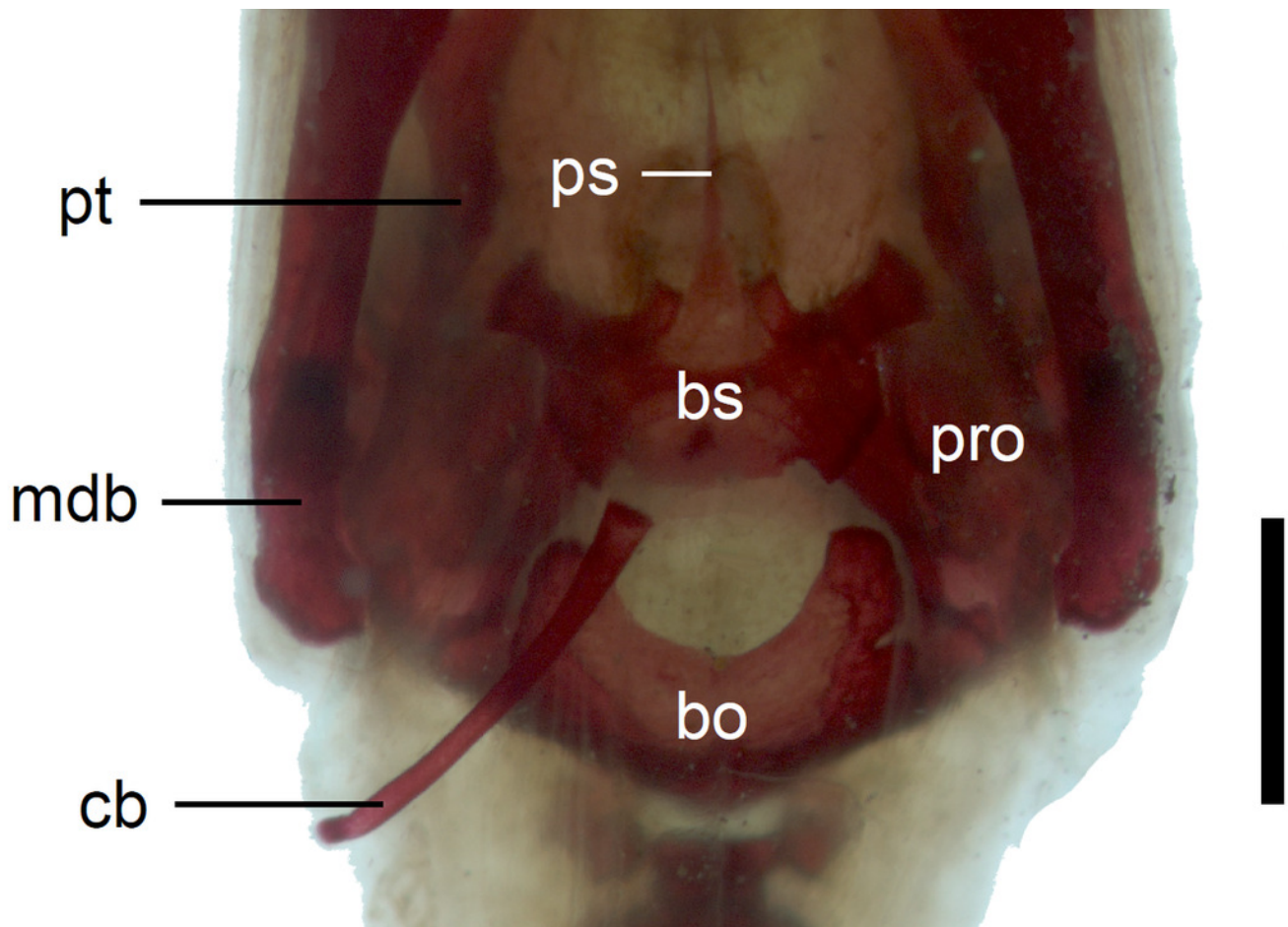
Figure 13

Skull of perinatal *Anguis fragilis* (MNHW-Reptilia-0312) in ventral view.

Scale bar = 2 mm. Abbreviations: bh, basihyal; bo, basioccipital; bs, basisphenoid; cb, first ceratobranchial; ch, ceratohyal; cl, clavicle; hh, hypohyal; Mc, Meckel's cartilage; pt, pterygoid.
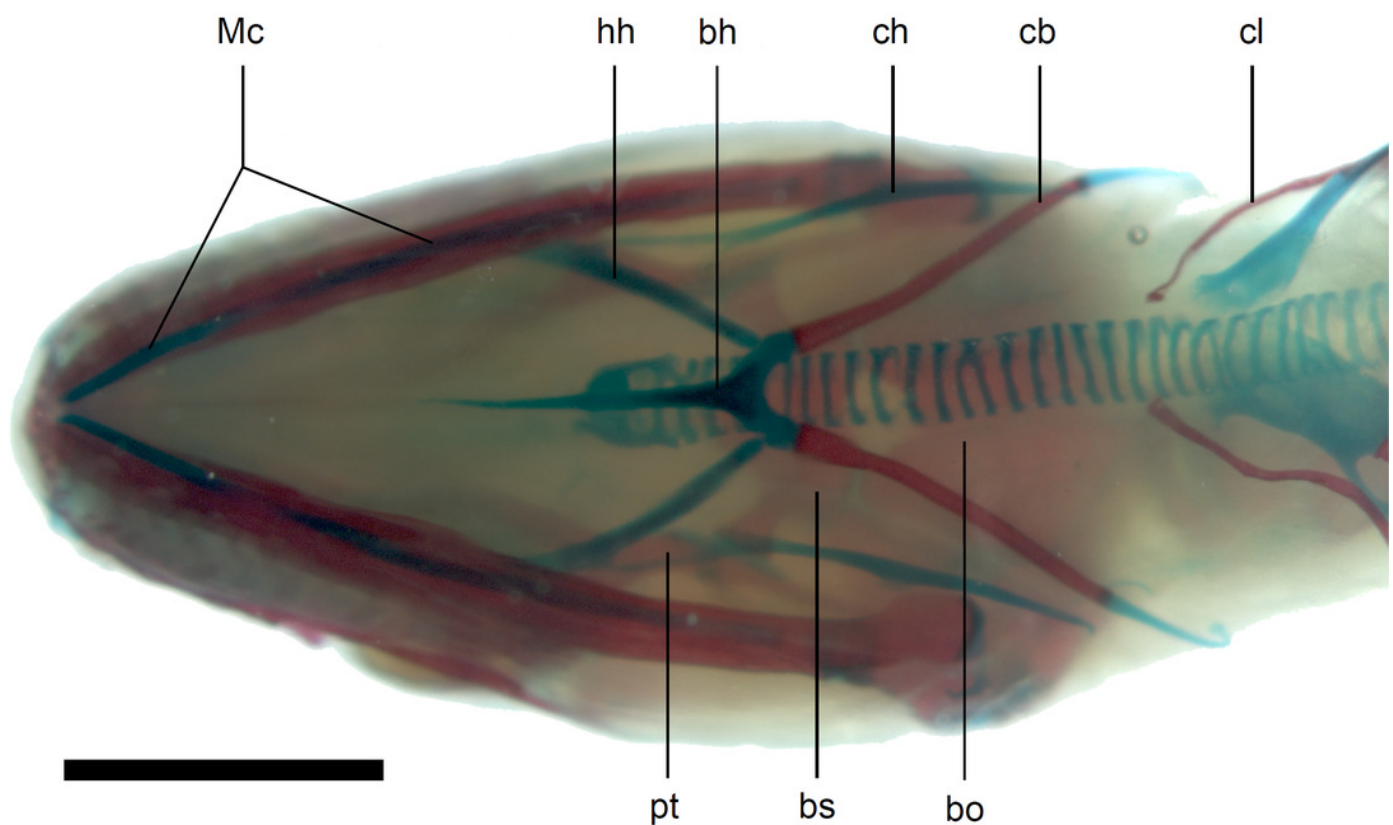
Figure 14

Pectoral girdle of perinatal *Anguis fragilis* (MNHW-Reptilia-0312) in lateral view.

Scale bar = 2 mm. Abbreviations: cl, clavicle; co, coracoid; eco, epicoracoid cartilage; ns, neural spine; sc, scapula.
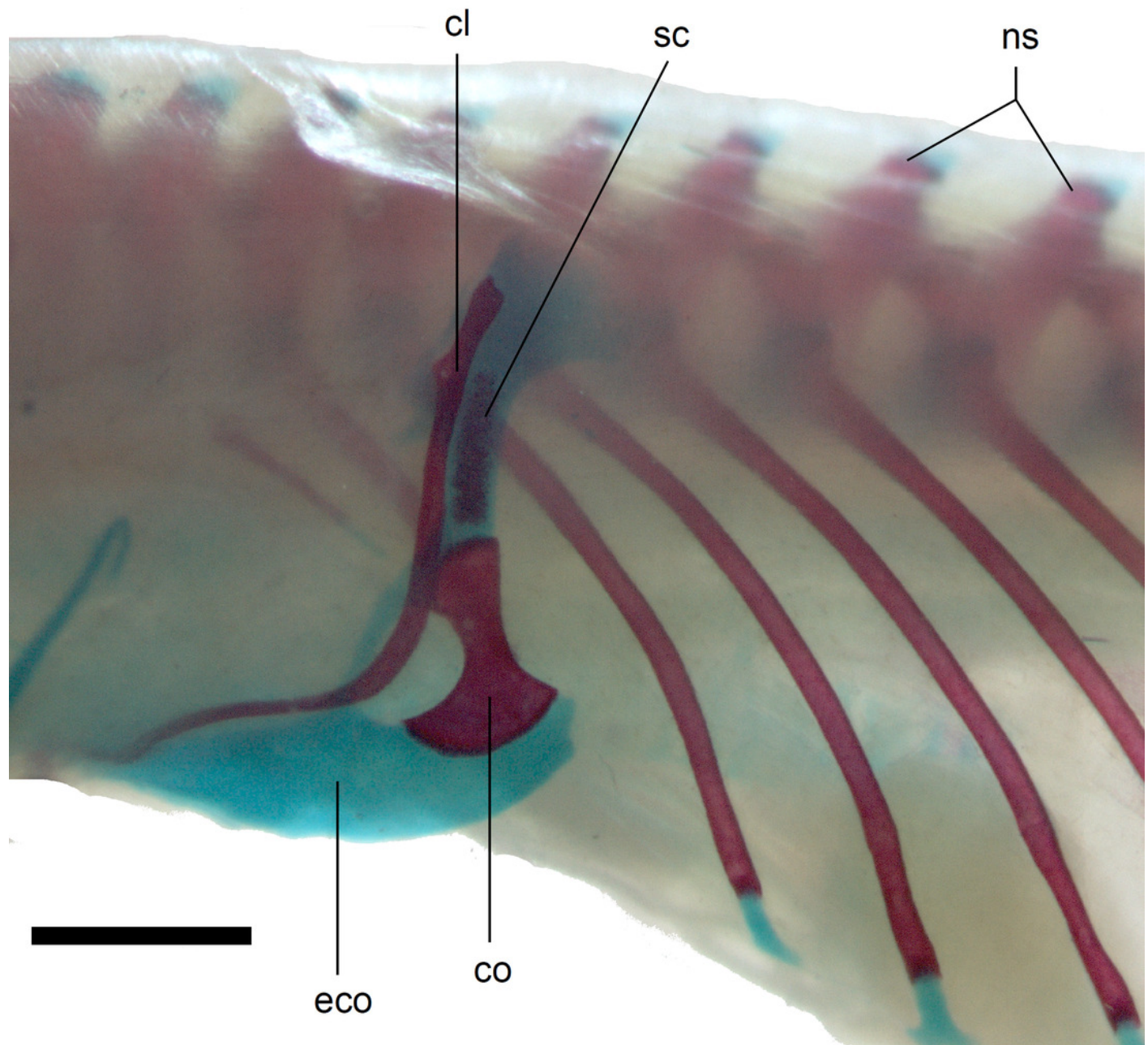
Figure 15

Pelvic girdle in perinatal *Anguis fragilis* in lateral view.

(A) MNHW-Reptilia-0311-1 (SVL = 49 mm). (B) MNHW-Reptilia-0312 (SVL = 55 mm). Scale
bar = 1 mm. Abbreviations: il, iliac process; is, ischiac process; pu, pubic process.
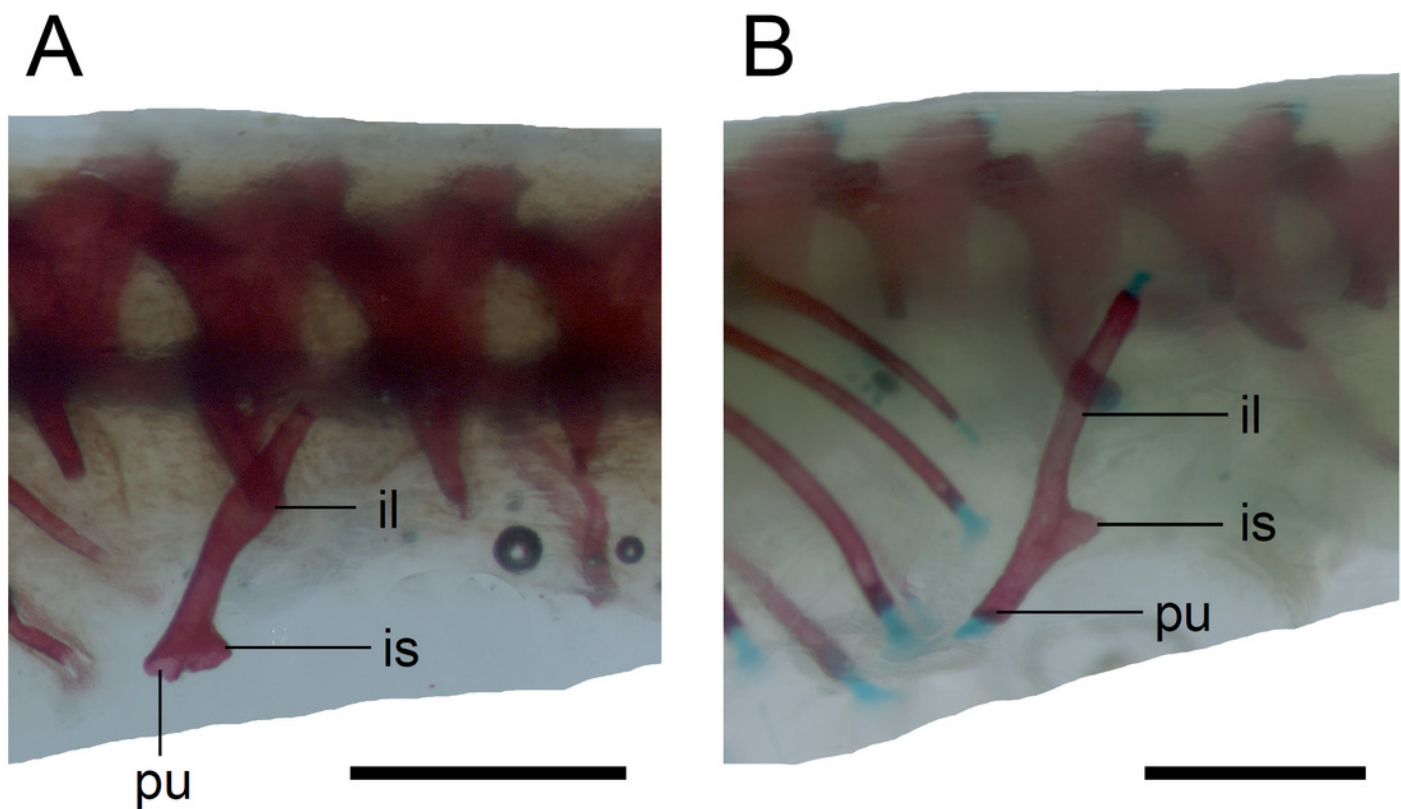
Basic information about analysed embryos of *Anguis fragilis*.

Female (catalogue number)	Snout-vent length	Date of collection	Collection site and coordinates	Number of embryos examined
MNHW-Reptilia-0251	152 mm	ca. July-August 2015	Pszczew 52.478 N, 15.780 E	8
MNHW-Reptilia-0316-3	143 mm	July 2016	Pszczew 52.478 N, 15.780 E	4
MNHW-Reptilia-0315-4	163 mm	9 July 2015	Bartniki 52.011 N, 20.250 E	2
MNHW-Reptilia-0315-5	177 mm	9 July 2015	Bartniki 52.011 N, 20.250 E	6
IZK 01007	Damaged specimen	Unknown	Unknown, presumably SW Poland	8
IZK 01008	Damaged specimen	Unknown	Unknown, presumably SW Poland	11
-	Unknown	Unknown	Unknown	3